

## **Developmental changes of functional and directed resting-state connectivities associated with neuronal oscillations in EEG**

**Lars Michels, Muthuraman Muthuraman, Rafael Lüchinger, Ernst Martin, Abdul Rauf Anwar, Jan Raethjen, Daniel Brandeis, Michael Siniatchkin**

### **Angaben zur Veröffentlichung / Publication details:**

Michels, Lars, Muthuraman Muthuraman, Rafael Lüchinger, Ernst Martin, Abdul Rauf Anwar, Jan Raethjen, Daniel Brandeis, and Michael Siniatchkin. 2013. "Developmental changes of functional and directed resting-state connectivities associated with neuronal oscillations in EEG." *NeuroImage* 81: 231-42. <https://doi.org/10.1016/j.neuroimage.2013.04.030>.

# Developmental changes of functional and directed resting-state connectivities associated with neuronal oscillations in EEG

Lars Michels<sup>a,b,\*</sup>, Muthuraman Muthuraman<sup>c,1</sup>, Rafael Lüchinger<sup>d</sup>, Ernst Martin<sup>a,e</sup>, Abdul Rauf Anwar<sup>c,f</sup>, Jan Raethjen<sup>f</sup>, Daniel Brandeis<sup>d,e,g,h,2</sup>, Michael Siniatchkin<sup>i,2</sup>

<sup>a</sup> Institute of Neuroradiology, University Hospital of Zurich, Zurich, Switzerland

<sup>b</sup> Center of MR-Research, University Children's Hospital, Zurich, Switzerland

<sup>c</sup> Digital Signal Processing and System Theory, Technische Fakultät Christian-Albrechts-Universität zu Kiel, Kiel, Germany

<sup>d</sup> Department of Child and Adolescent Psychiatry, University of Zurich, Zurich, Switzerland

<sup>e</sup> Zurich Center for Integrative Human Physiology (ZIHP), Zurich, Switzerland

<sup>f</sup> Department of Neurology, Christian-Albrechts-University of Kiel, Kiel, Germany

<sup>g</sup> Department of Child and Adolescent Psychiatry and Psychotherapy, Central Institute of Mental Health, Medical Faculty Mannheim/Heidelberg University, Mannheim, Germany

<sup>h</sup> Neuroscience Center Zurich, University of Zurich and ETH Zurich, Zurich, Switzerland

<sup>i</sup> Department of Child and Adolescent Psychiatry and Psychotherapy, Wolfgang Goethe-University of Frankfurt, Frankfurt am Main, Germany

## Introduction

The electroencephalography (EEG) has a long-standing tradition in human neurophysiology (Berger, 1930). EEG is one of the first techniques, which has been used to characterize the development of the human central nervous system. It has been demonstrated repeatedly that the absolute power of oscillations of the resting-state brain activity in lower frequency bands (delta (1–3 Hz), theta (4–7 Hz) and

lower alpha (8–10 Hz)) decreases exponentially with age, while power in higher EEG frequency bands (higher alpha (10–13 Hz) and beta (13–30 Hz)) shows less prominent decreases, or more complex changes such as an increase in childhood followed by a decrease during adolescence in the higher alpha band (Gasser et al., 1988; Lüchinger et al., 2011). Although these brain electric oscillations of different frequencies can be attributed to the activity of complex neuronal networks (Laufs, 2008), knowledge about structures which constitute these networks and how they are related to each other (functional connectivity), and about information flow within these networks (directed connectivity) is insufficient and sometimes ambiguous. Specifically, little is known about the normal development of functional and directed connectivities within networks underlying different oscillatory brain activities.

\* Corresponding author at: Institute of Neuroradiology, University Hospital of Zurich, Sternwartstr. 6, CH-8091 Zurich, Switzerland.

E-mail address: lars.michels@usz.ch (L. Michels).

<sup>1</sup> Shared first authorship.

<sup>2</sup> Shared senior authorship.

The most convincing studies on the function of neuronal networks and the link to oscillatory activity have been performed using simultaneous recordings of EEG and functional magnetic resonance imaging (fMRI) and correlating the absolute EEG power and changes of the blood oxygenation level-dependent (BOLD) signal. A regular observation is that the coupling strength between the EEG power and the BOLD signal is dependent on the examined frequency band as well as on the resting-state condition (Laufs et al., 2003; Mantini et al., 2007; Scheeringa et al., 2008). During the condition with eyes open (EO), EEG-fMRI studies in adults have found predominantly negative correlations for theta oscillations (Scheeringa et al., 2008) that is theta power increase is paralleled by BOLD signal decrease. During the condition with eyes closed (EC), several EEG-fMRI studies in adults have revealed negative correlations between alpha and beta power and BOLD signal changes predominantly in parieto-occipital regions as well as in the thalamus (Laufs et al., 2003). This is not surprising, as there is rich evidence from modeling and physiological studies for a fundamental role of alpha rhythm and thalamic activity (Lopes da Silva et al., 1974). Concerning developmental changes of neuronal networks of cortical oscillations, some studies have demonstrated that the resting-state coupling strength is almost identical between young adults and adolescents (Lüchinger et al., 2011) but differs between young adults and children (Lüchinger et al., 2012). Thalamic BOLD signal changes especially, were positively correlated to alpha and beta powers, yet stronger in adults than in children. Although EEG-BOLD signal correlations inform about state- and age-dependent interactions between the power fluctuations and the BOLD signal, they do not inform about the amount of synchronized oscillatory power in the space (and time) domain. A high level of synchronization between pairs of signals is considered to reflect structural and functional connections between cortical regions underlying the recording electrodes (Fein et al., 1988; Thatcher et al., 1986). One way to estimate synchronization in the frequency domain between neuronal activity, measured by EEG, magnetoencephalography (MEG), or fMRI, is the measurement of frequency-band specific coherence (Babiloni et al., 2004; Beaumont et al., 1978; Essl and Rappelsberger, 1998; Grasmann et al., 2004; Mizuhara et al., 2005; Sauseng et al., 2005; Schack et al., 1999; Sekihara et al., 2011; Srinivasan et al., 1998, 2007; Tucker et al., 1986). Several studies have been performed to describe task or rest-related coherence differences during childhood (Barry et al., 2004, 2005, 2009; Gasser et al., 1987, 2003; Knyazeva et al., 1994; Marosi et al., 1992) and adulthood (Anghinah et al., 2005; Clarke et al., 2008; Schellberg et al., 1990). Gasser et al. (1987) examined children during rest and visual task performance and found a moderate increase in coherence with age (between 10 and 13 years). In addition, there is evidence from resting MEG and EEG studies that coherence increases with age in healthy school-aged children especially in the delta and alpha bands (Marosi et al., 1992), but also shows a state-dependency (i.e., EO versus EC) in adults for ultraslow (<0.1 Hz) fluctuations (Liu et al., 2010).

Although the studies described above elucidate a specific frequency-dependent pattern of maturation by coherence, most studies only analyzed synchronization and coherences between scalp EEG signals. In contrast, dynamic imaging of coherent sources (DICS) is a tool to analyze networks of sources which may be attributed to any of brain oscillations obtained on the EEG or MEG (Gross et al., 2001; Kujala et al., 2008; Liljestrom et al., 2005; Moeller et al., 2012; Muthuraman et al., 2008, 2012a). The functional connectivity between sources may be represented by using coherence of source signals and the directed connectivity may be demonstrated by accessing information flow between sources using different methods of Granger causality, for example the renormalized partial directed coherence (RPDC) (Sameshima and Baccala, 1999; Schelter et al., 2009). Compared to other methods, there is increasing evidence that DICS may be able to demonstrate coherent changes not only between cortical sources, but even between cortical and very deep and subcortical structures, such

as the thalamus (Krause et al., 2010; Muthuraman et al., 2012a). This advantage of the RPDC method is especially relevant for the analysis of oscillatory brain activity, as it is frequently associated with activity in the thalamus (Butz et al., 2006; Krause et al., 2010; Moeller et al., 2012; Pollok et al., 2009). Both the coherences between cortical and subcortical sources of activity (functional connectivity) as well as the directionality of information flow between sources within networks underlying brain oscillations have not been investigated in studies which have dealt with maturation of brain oscillation (Takigawa et al., 1996; Varotto et al., 2010; Wang and Takigawa, 1992).

The aim of this study was to investigate the developmental changes of functional and directed connectivities within neuronal networks underlying different brain oscillations in healthy children and young adults. Since the frequency band power distribution differs between EC and EO we first asked whether, apart from spectral source mean power, frequency-band dependent coherence separates between EC and EO conditions in adults as well as in children. Since it is known from structural (Groeschel et al., 2010; McLaughlin et al., 2007; Whitford et al., 2007) and functional (Dosenbach et al., 2010b; Fair et al., 2007, 2008; Littow et al., 2010; Supekar et al., 2010) neuroimaging studies that certain cortical as well subcortical structures are not fully developed in children, we expected to see weaker regional coherence in children than in adults. We further asked whether directed coherence measured by EEG could index age and/or regional specific effects.

## Methods

### Subjects

Seventeen adults (mean age  $25.1 \pm 3.8$  years, 8 males) and 17 children (mean age  $10.1 \pm 1.3$  years, 9 boys), all right-handed with normal vision, were included in this study. Sex distributions did not differ between the two age groups (Pearson  $\chi^2$  (1,  $N = 34$ ) = 0.48  $p = 0.49$ ). All participants were healthy, with no history of medical or psychiatric disease, and were not currently taking drugs or medication. All children were enrolled in typical school programs and reported no special educational considerations. The group-specific IQ was not different between adults and children (adults: range: 98 to 137, mean IQ: 112.2; children: range: 98 to 130.5 mean IQ: 109.4). All participants as well as the parents/caregivers of the children gave written informed consent prior to participation. The study was approved by the local ethics committee. Subjects received a voucher for their participation in the study. EEG examinations in all subjects were performed in the early afternoon.

### Proceedings and EEG recordings

The EEG was recorded simultaneously with functional MRI during resting state condition for 10 min with alternating EO and EC blocks of 2.5 min. 64 sintered Ag/AgCl ring electrodes were attached using the "BrainCap" (Falk-Minow Services, Herrsching-Breitbrunn, Germany), which is part of the MR-compatible EEG recording system "BrainAmp-MR" (Brain Products Co., Gilching, Germany). Electrode impedance was kept below 10 k $\Omega$  (after subtraction of the value of the safety resistors). EEG montage was based on a selection of 10–20 system positions (Brem et al., 2010). Two additional electrodes were used to record eye movements and two further electrodes were used to obtain the electrocardiogram. F1 served as recording reference, and F2 was the ground electrode. Data were transmitted from the high-input impedance amplifier (250 Hz low-pass filter, 10 s time constant, 16-bit resolution, 32 mV dynamic range), which was placed directly behind the head coil inside the scanner room and connected to a computer located outside the scanner room via a fiber optic cable. The scanner (10 MHz clock output) was synchronized with the EEG amplifier (5 kHz sampling rate). Online correction of gradient artifacts

based on the averaged artifact subtraction algorithm was performed using RecView software (Brain Products Co., Gilching, Germany) enabling visual inspection of EEG.

### EEG analysis

EEG preprocessing and analysis were done using Brain Vision Analyzer 1.05 (Brain Products, Gilching, Germany). MR-gradient artifacts were removed by average artifact subtraction (Allen et al., 1998, 2000) with a sliding average over 50 TRs. To eliminate the ballistocardiogram artifact a very similar subtraction procedure was used, with the artifact window aligned on QRS complexes detected in the electrocardiogram (ECG) traces (templates based on 10 consecutive pulse intervals and individually-estimated time delay for subtraction based on global field power distribution). EEG was digitally bandpass-filtered (0.5–70 Hz, 24 dB/oct and 50 Hz Notch) and further downsampled to 256 Hz. An infomax ICA (Delorme and Makeig, 2004) was calculated on the concatenated data sets of the two resting session. Components were profiled by their topography, activation time course, spectrogram, and contribution to averaged BCG amplitude. Components clearly assigned to either eye blinks (Jung et al., 2000), residual MR-gradient or BCG artifacts were excluded from the back projection. For all groups, the mean overall data length after these pre-processing steps ranged between 8 and 10 min but did not differ between groups ( $p > 0.05$ , two-tailed paired  $t$ -test). All channels (electrooculogram (EOG) and ECG channels were excluded) were then transformed to the average reference (Lehmann and Skrandies, 1980), and EEG segments with remaining artifacts were removed. The EEG data set of each participant was then parsed into EO and EC conditions. Each condition onset was defined individually by the exact time of eye opening and closing, respectively, as indicated by ICA component activation trace. Next, the power spectral density was estimated for each condition, whereby the EEG signal was parsed in 2 s windows. For each of these segments a fast Fourier transformation (FFT, hamming window: 10%, frequency resolution of 0.25 Hz) was computed electrode-wise and averaged across segments. The average band power was calculated as the integrated area under the absolute power spectrum in the specific frequency band of interest, divided by the width (in points) of the specific frequency band. For the spectral band source mean power and synchronization analysis (see below) across all sources, the following frequency bands were examined: delta (1–3 Hz), theta (4–7 Hz), alpha (8–13 Hz), and beta (14–30 Hz).

### Analysis of coherent sources

The total interaction strength, which is the mean coherence between all the sources during the EC and EO condition, was analyzed using DICS (Gross et al., 2001). The basis of the source analysis (DICS) is the so-called beamforming approach (Hillebrand et al., 2005; Pascual-Marqui et al., 2009; Sekihara and Scholz, 1996). There are two major constraints in this beamformer DICS analysis: it assumes a single dipole model, which is not linearly correlated to other dipoles and the signal-to-noise ratio is sufficiently high (Gross et al., 2001). To determine coherence between brain areas, the spatial maximum of the power was identified and then defined as the seed region. Here the assumption is that the coherence between the reference and itself is always 1. In the next step this area of the brain or the activated voxels are considered as noise in order to find further coherent areas in the brain (Schoffelen et al., 2008). The selection of the reference region and the subsequent network sources was done on an automatic basis. The output of the beamformer at a voxel in the brain can be defined as a weighted sum of the output of all EEG channels (Van Veen et al., 2002). The beamformer weights for a given source (at a location of interest) are determined by the data covariance matrix and the forward-solution (lead-field matrix – LFM). The lead-field matrix was estimated with specified models for the brain. In this study, the

brain was modeled by a more complex, five-concentric-sphere model (De Munck, 2002; van Uitert and Johnson, 2000) with a single sphere for each layer corresponding to the white matter, gray matter, cerebral spinal fluid, skull and skin. The volume conductor model was created using standard T1-weighted magnetic resonance images. Part of the forward modeling and the source analysis was done using the open source software FieldTrip (Oostenveld et al., 2011). For both groups, the head was modeled using the radius and the position of the sphere with the standard electrode locations, that is, the same head model was used for children and adults. The LFM contains the information about the geometry and the conductivity of the model. The complete description of the solution for the forward problem has been described previously elsewhere (Muthuraman et al., 2010).

The weights determine the spatial filtering characteristics of the beamformer and are selected to increase the sensitivity to signals from a voxel and reducing the contributions of the signals from (noise) sources at different locations. The frequency components and their linear interaction are represented as a cross-spectral density (CSD) matrix. The two measures which can be derived from the CSD matrix are power and coherence. Coherence can be estimated by normalizing the CSD between two signals with their power spectral densities. In order to visualize power and coherence in the brain at a given frequency range, a linear transformation is used based on a constrained optimization problem which acts as a spatial filter (Van Veen et al., 2002). The brain region representing the strongest power in a specific frequency band can subsequently be used as a reference region for cortico-cortical coherence analysis. Areas were selected by a within-subject surrogate analysis to define the significance level, which was then used to identify areas in the brain as activated voxels as noise for subsequent runs of the source analysis. In order to create tomography maps, the spatial filter is applied to a large number of voxels covering the entire brain using a voxel size of 5 mm. Once coherent brain areas were identified, their activity was extracted from the surface EEG (source space).

In a further analysis, all the original source signals for each source with several activated voxels were combined by estimating the second order spectra and employing a weighting scheme depending on the analyzed frequency range to form a pooled source signal estimate for each source as previously described (Amjad et al., 1997; Rosenberg et al., 1989). The individual maps of coherence were spatially normalized and interpolated on a standard T1 brain in SPM2 (Wellcome Trust Centre for Neuroimaging). The application of the spatial filter has been described elsewhere (Muthuraman et al., 2008). This analysis was performed for each subject separately, followed by a grand average across all children and adults separately for the EC and EO conditions.

### Directionality analysis

Coherence only reveals components that are mutually correlated to two signals in the frequency domain. It does not give the direction of information flow between two signals. Renormalized partial directed coherence (RPDC) is a technique, based on the perspective of Granger causality (time domain), performed in the frequency domain to detect causal influences (i.e., directed connectivity) in multivariate stochastic systems and provides information on the direction of information flow between the source signals (Schelter et al., 2009). The multivariate model was based strictly on causality (i.e., not taking into account zero-lagged or instantaneous influences) and was used to model the pooled source signal estimates by an autoregressive process to obtain the coefficients of the signals in the defined frequency band. The open source Matlab (The MathWorks, Inc., Natick, MA, USA) package ARFIT (Arnold and Tapio, 2001; Tapio and Arnold, 2001) was used to estimate the autoregressive coefficients from the spatially filtered source signals. The correct model order required for the determination of these coefficients was estimated by minimizing the Akaike information criterion (AIC) (Akaike, 1974). The AIC is a measure of the relative goodness of

fit which has the minimum loss of information of a resulting statistical model with an optimal order for the corresponding model (Ding et al., 2000). After estimating the RPDC values the significance level was calculated from the applied data using a bootstrapping method (Kaminski et al., 2001).

Since the information flow between brain areas is difficult to estimate from EEG measurements due to the presence of noise and bias of volume conduction (Nolte et al., 2004), any effective connectivity measure (here RPDC) has to be carefully tested for its reliability to detect the underlying neuronal interactions during any functional state of interest (here resting state). In this context, some authors used the imagery part of coherence (Dubovik et al., 2012; Nolte et al., 2004) or time reversal technique (TRT) (Haufe et al., 2013). In a recent simulation study, Haufe et al. (2013) showed that the TRT is an appropriate method to alleviate the influence of weak asymmetries (i.e. non-causal interactions caused by zero-lagged, instantaneous coherences (= volume conduction)) on the result of any causal measure, while maintaining or even amplifying the contribution of strong asymmetries (i.e. time-lagged causal interactions not caused by volume conduction). Thus, we applied TRT as a second significance test on the connections already identified by RPDC using bootstrapping as a data-driven surrogate significance test. According to the TRT approach, if a uni-directional information flow between two time series, namely from A to B, is due to strong asymmetry, then a time reversal of time series A and B (i.e., a recalculation of the RPDC values) should reverse the result. The same logic holds for bi-directional information flow between two time series. The TRT approach is illustrated in Fig. 1. In general, for the multivariate autoregressive model of RPDC any directional information flow between the two signals  $x(t)$  and  $y(t)$  can be computed by:

$$x(t) = a_1 * y(t-1) + \eta(t)$$

where the time lagged term  $y(t - 1)$  (i.e., strong symmetries) influences  $x(t)$ , which is being governed by  $a_1$ . Due to this model, lagged coherence  $y(t)$  can contribute to the information flow towards  $x(t)$ , restricting any instantaneous causality (e.g. volume conduction, weak symmetries). In contrast, volume conduction effects are attributed to the noise term  $\eta(t)$  since it captures any weak asymmetries. This noise term is needed to estimate RPDC. However, our calculation of RPDC asymmetries eliminates this noise term, which is constant across directions and TRT. Accordingly, the RPDC asymmetries should be insensitive to contributions from volume conduction or other instantaneous interactions. In addition, our RPDC asymmetry calculation should completely revert by applying TRT, and therefore be only sensitive to strong causal interactions during brain development and adulthood. We applied TRT on the RPDC values for both states (EO and EC) and groups (adults and

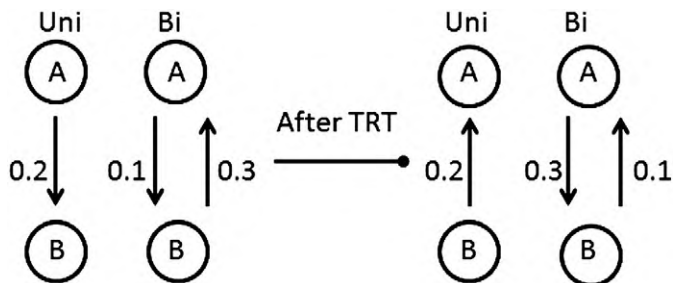


**Fig. 1.** Illustration of the time reversal technique (TRT). The TRT approach assumes that if a uni-directional information flow (“Uni”) between two time series from A to B is due to strong asymmetry (= causal interactions), then a time reversal of time series A and B should give identical results but in the opposite direction from B to A. The same logic holds for a bi-directional information flow (“Bi”) between two time series, where the two RPDC values (one per direction) will interchange with their counterparts.

children) and compared these results with results of RDPC analysis without TRT.

### Statistical analysis

Spectral source mean power differences within the different frequency bands of interest were assessed by two-tailed paired t-tests. The significance of the sources was tested by a within-subject surrogate analysis. The surrogates were estimated by a Monte Carlo random permutation 100 times shuffling of one-second segments within each subject. The p-value for each of these 100 random permutations was estimated and then the 99th percentile p-value was taken as the significance level in each subject (Muthuraman et al., 2012a). To ensure that any of the reported results (which are all calculated for pre-defined frequency bands) are not confounded by group differences in individuals' alpha frequency (IAF), we also estimated and compared individual band limits calculated as a percentage of the IAF (Doppelmayr et al., 1998). First, we calculated the IAF from the mean of all EEG channels excluding EOG and ECG channels. Next, based on the IAFs, we defined the lower and upper boundaries of the other frequency bands (delta, theta, and beta) within 10% of the predefined band edges. For example, one adult subject had an IAF of 10.1 Hz, so the lower band edge for the delta band (defined as 1–3 Hz) is 1.01 Hz ( $0.1 (10\% \text{ of } 1 \text{ Hz}) \times 10.1 \text{ Hz}$ ) and the upper edge is 3.03 ( $0.3 \times 10.1 \text{ Hz}$ ). We then estimated the median frequency band values for all subjects to see whether those values lie in the range of the pre-defined frequency band, and whether the values differ within a group (one-sample t-tests) and between groups (paired t-tests).

Next, for the statistical comparison on the coherence values, the mean coherence (or interaction strength) between all the sources was estimated for testing the significance between children and adults. A Friedman two-way analysis of variance test was then performed on the mean coherence values. In order to find the difference in coherence strength between the EC versus EO within adults and within children separately a Friedman two-way analysis of variance test was performed with the coherence values on the first source from each subject. Between-group coherence differences were assessed as follows: First, a reference voxel was selected in the posterior parietal cortex with the MNI co-ordinates [8, -77, 38]. The criteria for picking up this voxel were first to identify the voxel, which was activated the most in the identified first source in the network of sources. Secondly, the identified voxel should be from the first identified sources over all the conditions. Thirdly, the voxel should have the lowest power in all frequency bands. As mentioned above, the standard head model was used for both groups, which give the advantage of selecting the same reference voxel across children and adults. Within this spatial template, the Euclidean distance was estimated between the reference voxel and the voxel with the maximum power or coherence for the maximal overlapping number of sources between both groups for all sources.

The quantitative measure of distance was then compared group-wise between the children and adults for each source with a t-test of unrelated samples. Specifically, any significant between-group effect does reflect differences in the Euclidean distances between the reference voxel and (particular) group-overlapping sources.

For the between group analysis on the RPDC values, the same reference voxel was chosen as described above. Next, the directionality or information flow was estimated between this and the maximally activated voxel of all sources. The RPDC values were then compared between the two groups with a two-tailed t-test of unrelated samples. The hypothesis is that the directionality between the reference voxel and the maximally activated voxel for each source is different between the two groups. Since the directionality can be bi-directional (i.e., from the reference voxel to the maximally activated voxel and vice versa), we will report the subsequent results for both possible directions.

For all statistical analyses, the significance level was kept at  $p < 0.001$ .

## Results

### Analysis of individual median frequency band values and source spectral absolute mean power

The IAF was not different between adults and children (i.e.  $IAF_{(adults)}$ : 10.7 Hz,  $IAF_{(children)}$ : 10.28 Hz,  $p = 0.087$ ). Further, within-group (one-sample t-tests) and between-group (paired t-tests) median frequency band values were not different (supplementary Fig. 1). Based on these findings, all results will be reported according to the pre-defined frequency bands. For both resting states, spectral source mean power in the delta, theta, and alpha bands was higher for children (Fig. 2, black bars) than adults (Fig. 2, gray bars). No significant group difference was found for beta source power during EC and EO conditions, although the sign pointed to the same direction. The statistical analysis of global spectral mean EEG power differences between both groups is shown in supplementary Fig. 2.

### Analysis of coherent sources

Fig. 3 shows the results of the analysis of significant coherent ( $p < 0.001$ ) sources for children (A and B) and adults (C and D) for

EC and EO, and for all frequencies analyzed. Supplementary Figs. 3 (children) and 4 (adults) provide a more detailed summary of significant within-group between-source interactions during EC and EO.

In children, EC was related to the following pattern of coherence (Fig. 3A): delta activity was associated with sources in the posterior cingulate cortex (source 1, BA 26, 29, 30 & 31), primary motor cortex (source 2, BA4), and inferior frontal gyrus (source 3, BA44); theta activity was associated to sources in the parietal cortex and precuneus (source 1, BA39 and BA7), medial prefrontal cortex (source 2, BA9), and dorso-lateral prefrontal cortex (source 3, BA46); alpha activity correlated with sources in the parietal cortex (source 1, BA39), insula (source 2, BA16), visual cortex (source 3, BA17), medial and dorso-lateral prefrontal cortices (source 4, BA9 and BA46), inferior frontal gyrus (source 5, BA44), as well as thalamus (source 6, BA23); and beta activity correlated with sources in the visual cortex (source 1, BA17), middle cingulate cortex (source 2, BA23), posterior parietal cortex (source 3, BA7), dorso-lateral prefrontal cortex (source 4, BA46), medial prefrontal cortex (source 5, BA9), as well as thalamus (source 6, BA23).

For EO (Fig. 3B), delta activity was associated with sources in the medial and dorso-lateral prefrontal cortices (source 1, BA9 and BA46), temporal cortex (source 2, BA20) and posterior parietal cortex (source 3, BA7); theta activity was related to sources in the middle cingulate cortex and premotor cortex (source 1, BA32 and BA6), medial and lateral prefrontal cortices (source 2, BA9 and BA10), as well as parietal cortex (source 3, BA39); alpha activity was attributed to sources in the occipital

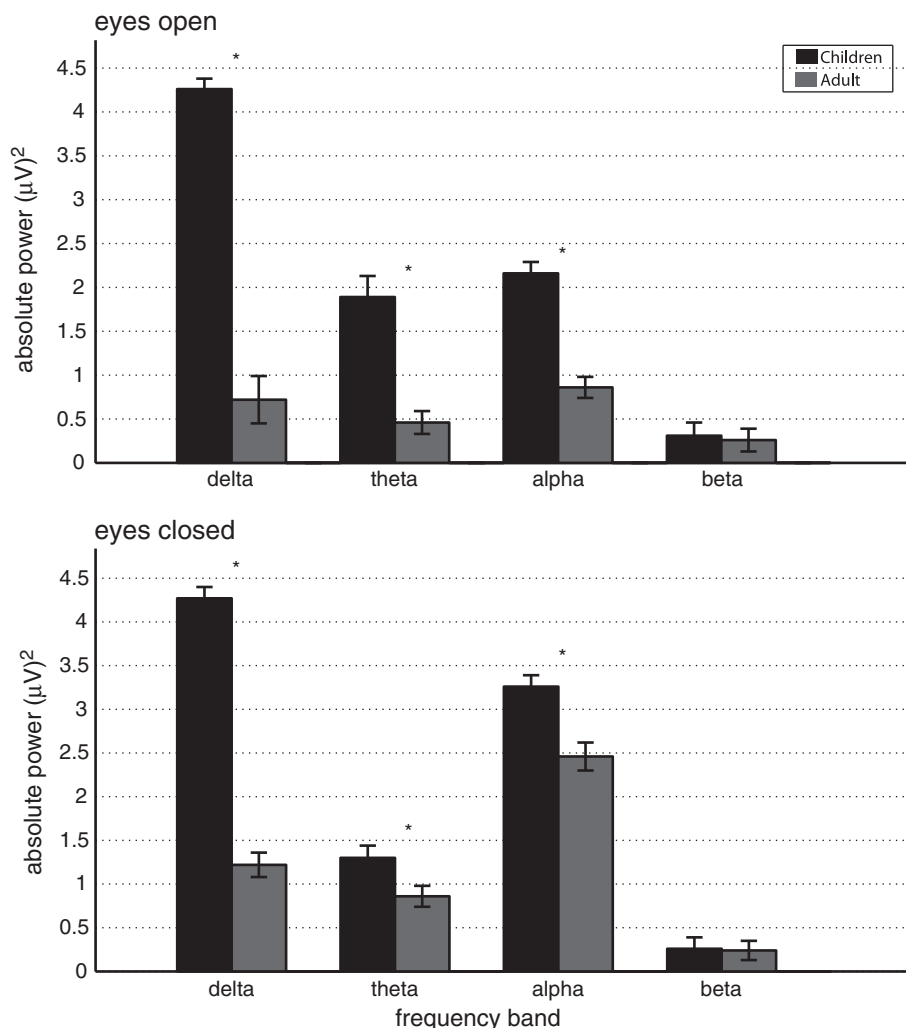
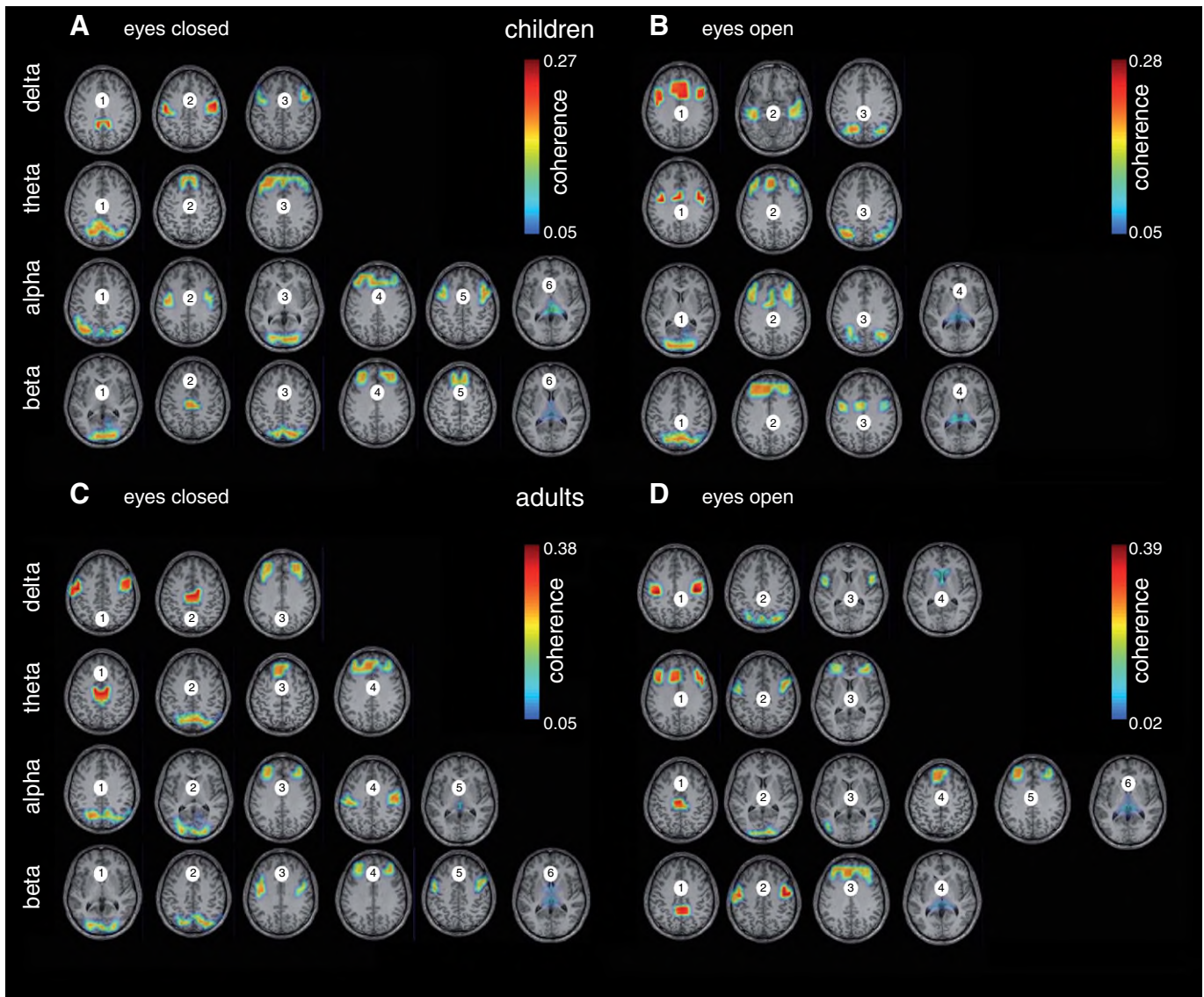


Fig. 2. Results of the spectral source power band analysis for eyes open and eyes closed conditions. Mean band power (with standard deviation) is shown for children (black bars) and adults (gray bars). Significant group differences are indicated by \* ( $p < 0.001$ ).



**Fig. 3.** Results of the frequency-band specific analysis of significant ( $p < 0.001$ ) coherent sources for children (A and B) and adults (C and D) for eyes closed and eyes open.

cortex (source 1, BA17); medial and dorso-lateral prefrontal cortices (source 2, BA9 and BA46); parietal cortex (source 3, BA39) and thalamus (source 4); and beta activity was correlated with sources in the parietal cortex and precuneus (source 1, BA39 and BA7), prefrontal cortex (source 2, BA46), middle cingulate cortex and premotor cortex (source 3, BA32 and BA6), as well as thalamus (source 4). There were no significant differences in the strength of coherence between conditions EC and EO in children ( $p = 0.64$ ).

For adults, delta activity was associated with coherent sources in the premotor cortex (source 1, BA6), middle cingulate cortex (source 2, BA32) and dorso-lateral prefrontal cortex (source 3, BA46) as shown in Fig. 3C; theta activity was related to the sources in the middle cingulate cortex (source 1, BA32), parietal cortex and precuneus (source 2, BA39 and BA7), medial prefrontal cortex (source 3, BA9) and dorso-lateral prefrontal cortex (source 4, BA46); alpha activity was attributed to the sources in the parietal cortex and precuneus (source 1, BA39 and BA7), occipital cortex (source 2, BA17), dorso-lateral prefrontal cortex (source 3, BA46), motor cortex (source 4, BA4), and thalamus (source 5, BA23); and beta activity correlated with sources in the occipital cortex (source 1, BA17), parietal cortex and precuneus (source 2, BA39 and BA7), premotor cortex (source 3, BA6), dorso-lateral prefrontal cortex

(source 4, BA46), inferior frontal gyrus (source 5, BA44), as well as thalamus (source 6).

During EO (Fig. 3D), the neural oscillations in adults were related to the following sources as following: delta activity was associated with sources in the premotor cortex (source 1, BA6), parietal cortex (source 2, BA39), insula (source 3, BA16), and caudate nuclei (source 4); theta activity was related to source in the medial and lateral prefrontal cortices (source 1, BA9 and BA10), inferior frontal gyrus (source 2, BA44), as well as orbitofrontal cortex (source 3, BA11); alpha activity was attributed to sources in the middle cingulate cortex (source 1, BA32); occipital cortex (source 2, BA17), parietal cortex (source 3, BA39), medial prefrontal cortex (source 4, BA9), dorso-lateral prefrontal cortex (source 5, BA46), and thalamus (source 6); and beta activity correlated with sources in the middle and posterior cingulate cortex (source 1, BA30 and BA31), premotor cortex (source 2, BA6), medial and dorso-lateral prefrontal cortices (source 3, BA9 and BA46) and thalamus (source 4).

As for children there were no significant differences in the strength of coherence between EO versus EC in adults ( $p = 0.57$ ). However, it seems likely that opening the eyes has an impact on the results of the source analysis as the visual inspection revealed different frequency-band specific coherent sources for EO than for EC.

In summary, the source analysis demonstrated that children were characterized by significantly higher spectral source mean power in all frequency bands except for the beta band (Fig. 1). In case of the total interaction strength, adults showed significantly higher mean coherence values in all frequency bands compared to children (Tables 1 & 2).

These observations were confirmed by the group statistics. There was a significant between-group difference ( $p < 0.001$ ) for most sources in all frequency bands for EO and EC conditions. However, some sources in alpha (source 1, EO), beta (sources 1 and 4 in EO and source 1 in EC), and theta (source 3, EC) frequency bands were not significantly different between the two groups, probably because these sources have the maximally activated voxel at the same location for both children and adults (see Fig. 3). A summary of between-group differences is shown in Table 3A.

### Directionality analysis

The information flow between sources (same naming as in Fig. 2) of brain activity for each frequency analyzed is illustrated in Fig. 4. In the following paragraph we will discuss only differences in the RPDC between groups.

In children, a unidirectional and cortical information flow was observed from prefrontal to parieto-occipital brain sources for the delta and theta bands for both EC and EO.

In adults, the same frequency bands showed a unidirectional information flow but in the opposite direction (from parieto-occipital to fronto-central brain regions). For alpha and beta, two different information flow patterns occurred in children: As for delta and theta, cortical information flow followed rather a posterior to anterior information flow (i.e. parieto-occipital sources connected to more central and frontal sources). Second, thalamo-cortical information flow between sources was always bilateral and widespread (i.e. not only observable between anterior sources and the thalamus).

The cortico-cortical information flow followed a parieto-occipital to fronto-central gradient in adults. However, in contrast to children, adults demonstrated only a unidirectional thalamo-cortical information flow, which originated from the thalamus. There were no notable differences in information flow between EO and EC in either group of subjects. Next, we analyzed whether within-group differences are robust against potential volume conduction effects. Here, the TRT analyses underlined the solidity of the above-mentioned results, as all significant causal interactions identified by RDPC were identified by the TRT as well (Supplementary Fig. 5).

Finally, there was a significant between-group difference in the directionality ( $p < 0.01$ ) for all frequency bands and sources irrespective of the resting state (Table 3B).

## Discussion

This study revealed the following main findings: On the spectral level, children showed stronger source mean power in all examined frequency bands compared to adults. On the level of functional connectivity, adults were characterized by significantly higher mean coherence between sources underlying oscillatory brain activity at rest than children in all frequency bands. The directed connectivity analysis revealed an

**Table 1**

The mean coherence values between all the sources from all subjects (separately for children and adults) for the condition EC.

| Coherence (mean) | Child | Adult             |
|------------------|-------|-------------------|
| Delta            | 0.25  | 0.31 <sup>a</sup> |
| Theta            | 0.21  | 0.27 <sup>a</sup> |
| Alpha            | 0.17  | 0.23 <sup>a</sup> |
| Beta             | 0.17  | 0.23 <sup>a</sup> |

Eyes closed (all sources).

<sup>a</sup> Indicates a significant group differences at  $p < 0.001$ .

**Table 2**

The mean coherence values between all the sources from all subjects (separately for children and adults) for the condition EO.

| Coherence (mean) | Child | Adult             |
|------------------|-------|-------------------|
| Delta            | 0.18  | 0.23 <sup>a</sup> |
| Theta            | 0.17  | 0.22 <sup>a</sup> |
| Alpha            | 0.17  | 0.24 <sup>a</sup> |
| Beta             | 0.18  | 0.25 <sup>a</sup> |

Eyes open (all sources).

<sup>a</sup> Indicates a significant group differences at  $p < 0.001$ .

anterior to posterior information flow (directed coherence) between cortical sources in children for the delta and theta EEG bands, while adults showed the opposite relationship. Most strikingly, for the alpha and beta band the thalamic source was a significant part of the network in both adults and children, however, the influence of the thalamus on cortical sources was found only in adults while children showed bidirectional thalamo-cortical flow of information. The between-group analysis confirmed that the group-specific coherence strength and information flow (directed coherence) was different between groups of subjects. This indicates that EEG measures of functional and directed coherence are sensitive to differences in brain maturation.

### Developmental differences in coherence

We found that the absolute source power from delta, theta, and alpha was significantly higher for children than for adults; a similar group difference did not reach significance in the case of the beta band. The results were also observed when using individual (i.e., IAF-based) band definitions (see Methods) rather than fixed pre-defined bands across both groups. These results are in line with numerous scalp EEG findings and especially with a recent EEG-fMRI study by our group (with a nearly identical group of subjects), for which we also found consistently stronger spectral scalp power in children than adults, particularly for the lower frequency bands (Lüchinger et al., 2011). This result indicates that the classical topographical maps usually obtained with EEG or MEG (e.g. parieto-occipital alpha during EC) are preserved in resting EEG-fMRI recordings as well. This is a prerequisite for the subsequent coherence analysis performed in this study, as any divergence in the spatial distribution of spectral power between resting EEG and EEG-fMRI would certainly not justify a comparison of literature-based EEG power and coherence effects with the results from the present (EEG-fMRI data driven) study.

Second, we found higher rest-related coherence values in adults compared with children in all frequency bands. There is a large body of evidence that developmental changes in the brain are predominantly determined by myelination and synaptogenesis (Huttenlocher, 1990; Yakovlev and Lecours, 1967). Myelination leads to efficient connections between cortical and subcortical brain regions. Specifically, it is known that synaptic density declines in the human brain starting at age 9–10 and continuing into early adulthood. This decrease can be captured by a number of brain imaging methods, such as PET (Chugani et al., 1987), MRI (Gogtay et al., 2004), and EEG. Using EEG or MEG it has been shown that coherence or more general synchronous neural activity is lower in children than in adults, as indexed by waking (Barry et al., 2004; Gasser et al., 1988; Segalowitz et al., 2010) and sleep EEG (Feinberg and Campbell, 2010; Tarokh et al., 2010). It seems likely that the DICS method reflects such developmental coherence effects at the source level as adults demonstrate overall stronger mean coherence values across sources. This observation of enhanced functional connectivity in adults is in line with fMRI data which shows a significant increase of the resting state functional connectivity between local and distant brain regions, especially in the fronto-parietal network (Fair et al., 2007).

Further, our resting state results parallel task related developmental findings, as we and others (Muller et al., 2009) found decreasing spectral

**Table 3**  
Summary of coherence (A) and directed coherence (B) differences between adults and children. In (A) negative t-values indicate shorter Euclidean distances between the reference voxel and particular, group-overlapping sources for children compared to adults. In (B), positive values in the column directionality indicate information from a given source to the reference voxel; negative values (i.e., -1) indicate information from the reference voxel to a given source. EO: eyes open, EC: eyes closed, freq: frequency.

| (A)   |       |        |         |         |       |       |        |         |         |
|-------|-------|--------|---------|---------|-------|-------|--------|---------|---------|
| State | Freq. | Source | t-Value | p-Value | State | Freq. | Source | t-Value | p-Value |
| EO    | Delta | 1      | 6.8     | <0.0001 | EC    | Delta | 1      | -31.6   | <0.0001 |
|       |       | 2      | 27.2    | <0.0001 |       |       | 2      | 9.8     | <0.0001 |
|       |       | 3      | -7.9    | <0.0001 |       |       | 3      | -8.7    | <0.0001 |
|       | Theta | 1      | -10.6   | <0.0001 |       | Theta | 1      | -5.4    | <0.0001 |
|       |       | 2      | 10.4    | <0.0001 |       |       | 2      | 28.2    | <0.0001 |
|       |       | 3      | -31.7   | <0.0001 |       |       | 3      | 1       | 0.31    |
|       | Alpha | 1      | -1.2    | 0.25    |       | Alpha | 1      | 2.9     | 0.007   |
|       |       | 2      | 18.9    | <0.0001 |       |       | 2      | 3.7     | 0.001   |
|       |       | 3      | -4.9    | <0.0001 |       |       | 3      | -36.6   | <0.0001 |
|       |       | 4      | -10     | <0.0001 |       |       | 4      | 18.3    | <0.0001 |
|       | Beta  | 1      | 0.13    | 0.9     |       | Beta  | 5      | 18.6    | <0.0001 |
|       |       | 2      | 13.9    | <0.0001 |       |       | 1      | -1.8    | 0.09    |
|       |       | 3      | -13.9   | <0.0001 |       |       | 2      | 12.1    | <0.0001 |
|       |       | 4      | 0.7     | 0.52    |       |       | 3      | -16.9   | <0.0001 |

| (B)   |       |        |                |         |         |       |       |         |                |         |         |
|-------|-------|--------|----------------|---------|---------|-------|-------|---------|----------------|---------|---------|
| State | Freq. | Source | Directionality | p-Value | t-Value | State | Freq. | Source  | Directionality | t-Value | p-Value |
| EC    | Delta | 1      | 1              | -9.9    | <0.0001 | EC    | Delta | 1       | 1              | -7.4    | <0.0001 |
|       |       | 2      | 1              | -6.9    | <0.0001 |       |       | 2       | 1              | -8.9    | <0.0001 |
|       |       | 3      | 1              | -9.9    | <0.0001 |       |       | 3       | 1              | -9.1    | <0.0001 |
|       |       | 1      | -1             | -17.5   | <0.0001 |       |       | 1       | -1             | -7.9    | <0.0001 |
|       |       | 2      | -1             | -5      | <0.0001 |       |       | 2       | -1             | -10.8   | <0.0001 |
|       |       | 3      | -1             | -2.5    | 0.02    |       |       | 3       | -1             | -7.4    | <0.0001 |
|       | Theta | 1      | 1              | -8.4    | <0.0001 |       | Theta | 1       | 1              | -8.2    | <0.0001 |
|       |       | 2      | 1              | -8      | <0.0001 |       |       | 2       | 1              | -7.1    | <0.0001 |
|       |       | 3      | 1              | -9      | <0.0001 |       |       | 3       | 1              | -8.8    | <0.0001 |
|       |       | 1      | -1             | -7.9    | <0.0001 |       |       | 1       | -1             | -8.8    | <0.0001 |
|       |       | 2      | -1             | -9.6    | <0.0001 |       |       | 2       | -1             | -9.2    | <0.0001 |
|       |       | 3      | -1             | -7.7    | <0.0001 |       |       | 3       | -1             | -7.2    | <0.0001 |
|       | Alpha | 1      | 1              | -7.5    | <0.0001 |       | Alpha | 1       | 1              | -6.5    | <0.0001 |
|       |       | 2      | 1              | -5.6    | <0.0001 |       |       | 2       | 1              | -8.9    | <0.0001 |
|       |       | 3      | 1              | -10.1   | <0.0001 |       |       | 3       | 1              | -8.5    | <0.0001 |
|       |       | 4      | 1              | -14.3   | <0.0001 |       |       | 4       | 1              | -14.2   | <0.0001 |
|       |       | 1      | -1             | -6.9    | <0.0001 |       |       | 5       | 1              | -9      | <0.0001 |
|       |       | 2      | -1             | -9.4    | <0.0001 |       |       | 1       | -1             | -9.4    | <0.0001 |
|       | Beta  | 3      | -1             | -9.9    | <0.0001 |       | 2     | -1      | -10.6          | <0.0001 |         |
|       |       | 4      | -1             | -10.5   | <0.0001 |       | 3     | -1      | -9.5           | <0.0001 |         |
|       |       | 1      | 1              | -6.9    | <0.0001 |       | 4     | -1      | -8.7           | <0.0001 |         |
|       |       | 2      | 1              | -7.8    | <0.0001 |       | 5     | -1      | -10.3          | <0.0001 |         |
|       |       | 3      | 1              | -8.9    | <0.0001 |       | Beta  | 1       | 1              | -8.4    | <0.0001 |
|       |       | 4      | 1              | -18.5   | <0.0001 |       |       | 2       | 1              | -7.1    | <0.0001 |
| 1     | -1    | -6     | <0.0001        | 3       | 1       | -10.1 |       | <0.0001 |                |         |         |
| 2     | -1    | -9.7   | <0.0001        | 4       | 1       | -14.3 |       | <0.0001 |                |         |         |
| 3     | -1    | -8.1   | <0.0001        | 5       | 1       | -8    |       | <0.0001 |                |         |         |
| 4     | -1    | -8.2   | <0.0001        | 6       | 1       | -9.6  |       | <0.0001 |                |         |         |
|       |       |        |                |         |         | 1     | -1    | -10.4   | <0.0001        |         |         |
|       |       |        |                |         |         | 2     | -1    | -11.8   | <0.0001        |         |         |
|       |       |        |                |         |         | 3     | -1    | -10.6   | <0.0001        |         |         |
|       |       |        |                |         |         | 4     | -1    | -11     | <0.0001        |         |         |
|       |       |        |                |         |         | 5     | -1    | -9.5    | <0.0001        |         |         |
|       |       |        |                |         |         | 6     | -1    | -9.8    | <0.0001        |         |         |

power with age, while at the same time global cortical synchronization was increasing during cognitive operations (Michels et al., 2012). Our findings can further be discussed in the context of more general current theories on the neural framework for EEG coherence, as the observed results lend support for a recent model, which proposed that a decline in (EEG) power and an increase in coherence are complementary processes that support cognitive gains during normal human brain development (Stevens, 2009). Therefore, we would argue that the successful integration of activity in anatomically distributed populations of neurons relies on increased coherence, assuming that neural function is indexed by short- and long-range coherence. Recently, it has been proposed that the presence of frequency-band specific functional integration by coherence can be achieved by neurons in distal regions – connected by axons – which synchronize their response temporally by oscillating at the same frequency (Singer, 2009). In this way, temporary networks

can be formed to serve a specific function and then dissolved to form new networks. We conclude that the higher cortico-cortical and coherence cortico-subcortical in adults reflects a complex neuronal interplay between widespread brain sources, which is not fully developed only in children.

#### *The direction of information flow during rest: Age-dependent differences*

The most striking finding of this study was that adults showed directed connectivity (assessed by RPDC) from parieto-occipital to frontal sources in all frequency bands, whereas children showed an opposite pattern of information flow, most pronounced in the delta and theta bands.

These findings were also confirmed by TRT, which showed a complete reversal of all significant asymmetries detected by RPDC (as expected for

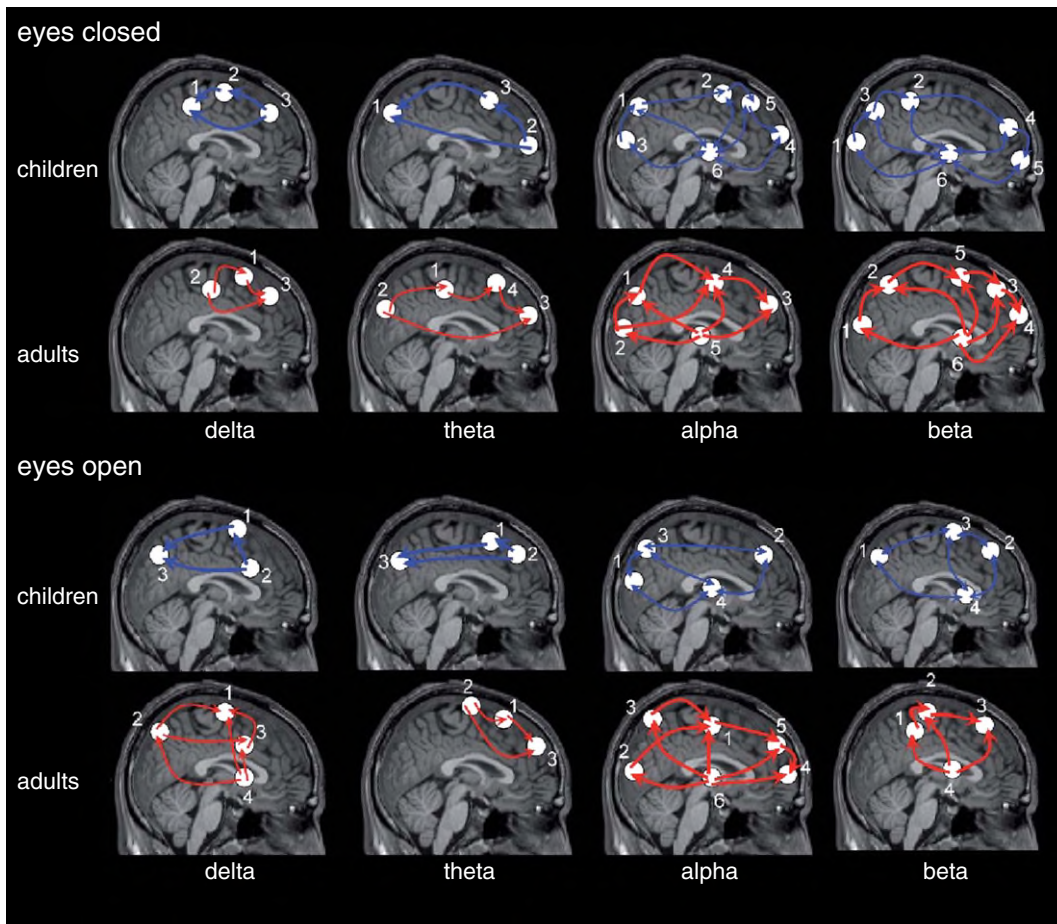


Fig. 4. Illustration of information flow between sources (same source naming as in Fig. 1) of brain activity for each frequency band.

strong asymmetries due to lagged coherence), suggesting that RDPC is a powerful technique to reliably detect resting-state related causal interactions during brain development. From EEG, it is known that coherence at frontal locations decreases with increasing age, most pronounced in the theta band, which might be the result of increased cortical differentiation (Thatcher et al., 1986). Our results support this notion, as directed connectivity in adults never originated in frontal sources in the two different resting-states. Yet, we additionally conclude that not only the coherence differs as a function of age but also the direction of information flow, as we found higher influence of parieto-central sources on frontal sources in adults compared to children.

The second major finding was that alpha and beta band coherence was present not only between different cortical sources but also between cortical and subcortical sources, namely the thalamus. There is rich evidence for the importance of thalamocortical connections mediating a crucial role in complex cognitive functioning (Van der Werf et al., 2003) and that those connections show functional and structural developmental changes (Alkonyi et al., 2011). Further, from resting functional connectivity fMRI studies it is known that several cortical regions are less connected in children than in adults (Dosenbach et al., 2010a; Fair et al., 2007, 2008) during low-cognitive operations (e.g., rest). Interestingly, we found exclusively unidirectional influences of the thalamus on cortical sources in adults. Several studies already demonstrated a tight coupling between alpha/beta band power and thalamic BOLD signal strength in adults (Goldman et al., 2002; Laufs et al., 2003, 2006; Moosmann et al., 2003). Of course we have to interpret our results with caution, as we do not know the underlying neural mechanism responsible for coherence or developmental coherence differences, respectively. Further, there are some uncertainties regarding EEG based localization of deep subcortical signals in the

presence of stronger cortical signals. In a recent EEG-fMRI study we demonstrated (in the same group of subjects) that EEG-BOLD signal correlations were nearly indistinguishable between children and adults, except for thalamic BOLD signal correlations with alpha- and beta power (Lüchinger et al., 2012). Thus, our study and other studies underline the relevance of the thalamus as an important relay station in the brain (Steriade and Deschenes, 1984; Steriade and Llinas, 1988), which might be indirectly described by directed coherence. It has recently been proposed that long-range coherence between distal (i.e., far away) sources at higher frequencies might be driven by a third region, namely the thalamus (Tarokh et al., 2010).

Further it was argued that coherence between proximal electrodes at low and high frequencies can result from cortico-cortical coupling or is driven by a third region. Although the information flow from the thalamus was widespread in both groups of subjects, the directed connectivity analysis revealed that the adults demonstrate exclusively, an outflow of information from thalamus to other cortical regions in lower and higher frequencies, while children demonstrate a bidirectional information flow between cortical regions and the thalamus. This might indicate that in children the thalamus requires feedback from cortical regions to operate properly. Recently, it has been observed in a spatial memory related fMRI study that healthy children (similar age range than in our study) show stronger functional connectivity between thalamo-striatal and thalamo-cortical loops compared to children with hyperactivity (Mills et al., 2012), suggesting that functional connectivity can label the level of brain maturation. However, there is also evidence that thalamocortical connectivity is not always increasing from child- and adulthood (Alkonyi et al., 2011). The authors reported in a DTI study that thalamic connectivity of some cortical regions showed a decrease with

age, while other regions (specifically the prefrontal cortex) demonstrate increasing thalamocortical connectivity with age. Recently, a study modeled the neurophysiological changes (within the delta-gamma bands) with age in a large group of healthy subjects ( $n = 1498$ ) aged 6–86 years, incorporating among other parameters, thalamocortical loops (van Albada et al., 2010). The authors found that neurophysiological changes in thalamocortical loops tend to be most rapid in childhood, generally leveling off at age 15–20 years. As we found in children, bidirectional connectivity between the thalamus and frontal, parietal as well as visual areas we would argue – based on the above-mentioned studies – that the observed bidirectional thalamo-cortical connectivity in children might reflect brain immaturity and that those connections will become fine-tuned (i.e., develop unidirectional connectivity) during adulthood. We want to emphasize that any observed unidirectional flow does not implicate that there is no bidirectional flow per se but only that the direction of information flow is stronger in one than in the other direction (asymmetric information flow).

#### *Coherence differences between eyes closed and eyes open states*

There is striking evidence that absolute and relative EEG/MEG power differs between EC and EO conditions, such as alpha power is particularly increased during EC acquisition. In addition, already in 1987 it was demonstrated that coherence values, estimated from EC power, exponentially increase in intra-hemispheric coherence between frontal and occipital EEG leads (Thatcher et al., 1987) with increasing age. Yet, it was not reported in which frequency band(s) this observation was made. We show that coherence values were generally higher during EC and EO in adults than in children. Further, it is evident that opening the eyes leads to a different involvement of neuronal sources, which suggests differences in integrity of the central nervous system dependent on sensory input. This resting-state dependent presence of neuronal sources was present in both examined groups. In fact, although the order of coherent source may differ between children and adults (Fig. 2), the localization of sources was very similar in both groups of subjects for the EC condition. However, for the EO condition, the localization of sources underlying brain oscillations differed substantially between adults and children. Thus, it seems likely that sensory input contributes to a large degree to heterogeneity of neuronal networks underlying brain oscillations.

#### *Limitations of the study*

Even though we could show age specific pattern of source coherence using DICS, this study also has some limitations. Firstly, the study revealed brain sources in deep brain structures such as thalamus. It is a matter of debate whether it is possible to find sources so deep in the brain based on recordings from the scalp. In previous MEG (Gross et al., 2001, 2002; Sudmeyer et al., 2006; Timmermann et al., 2003) and EEG (Muthuraman et al., 2012a) studies, subcortical sources have been detected by applying DICS to oscillatory signals (e.g. tremor), and also in healthy subjects during isometric contraction (Muthuraman et al., 2012b). Moreover, based on EEGs obtained simultaneously with functional MRI in patients with absence seizures and photoparoxysmal responses, DICS revealed sources in deep brain structures (thalamus) for oscillatory epileptic activity. The sources found in the thalamus corresponded with positive BOLD signal changes in thalamus in all patients. In contrast, there were no sources in the thalamus in patients who did not activate thalamocortical network during epileptiform discharges. In such a way, it was possible to validate the detection of sources in deep brain structures such as thalamus with another independent method with a better spatial resolution (Moeller et al., 2012). Secondly, in this study no realistic head models were used. Thus, the influence of age-related conductivity of head tissues resulting in differences in the lead field matrix on results of the DICS

cannot be excluded. Previous studies have demonstrated a clear advantage of MRI constrained spherical model, boundary element, as well as finite element models in localization of bioelectrical sources (Fuchs et al., 2007; Hallez et al., 2007). Although there is no doubt that realistic head modeling will possibly improve the localization power of DICS, we want to emphasize that conductivity differences in the examined age range can be considered as a minor factor to explain the observed group differences in directed connectivity, since only subtle differences in conductivity of the skull are found between the age 11 and 24 (Hoekema et al., 2003).

Although the current resting EEG was obtained during fMRI in the scanner, our spectral analysis clearly replicated all major developmental effects usually observed during EEG recordings outside of the MR scanner. Specially, for both source and scalp (Lüchinger et al., 2012) spectral power, we could replicate the standard spectral topographies and developmental patterns. Yet, the fact that slightly more ICA artifact components were excluded in children than adults (Lüchinger et al., 2012), due to stronger residual ballistocardiogram artifacts, is consistent with EEG findings outside the scanner, and suggests that the typical differences in EEG quality were well minimized.

#### **Conclusion**

This study demonstrates an age-specific pattern of (directed) connectivity, which may explain functional and behavioral differences in the context of human brain development. We thus conclude that both functional and directed connectivities are sensitive to brain maturation as the distribution and directionality of functional connections differ between the developing and adult brains.

#### **Acknowledgments**

This work has been supported by the University Research Priority Program “Integrative Human Physiology” (“Linking the major system markers for typical and atypical brain development: a multimodal imaging and spectroscopy study” and “Thalamocortical interaction in brain state regulation during normal development and in epilepsy”) at the University of Zurich. The funders had no role in study design, data collection and analysis, decision to publish, or preparation of the manuscript. Support from the ‘Deutsche Forschungsgemeinschaft’ (DFG, SFB 855) is gratefully acknowledged. We thank Dr. Arron Metcalfe and Dr. Ruth O’Gorman for their helpful comments on previous versions of the manuscript.

#### **Conflict of interest**

The authors have no conflicts of interest.

#### **References**

- Akaike, H., 1974. A new look at the statistical model identification. *IEEE Trans. Autom. Control* 19, 716–723.
- Alkonyi, B., Juhasz, C., Muzik, O., Behen, M.E., Jeong, J.W., Chugani, H.T., 2011. Thalamocortical connectivity in healthy children: asymmetries and robust developmental changes between ages 8 and 17 years. *AJNR Am. J. Neuroradiol.* 32, 962–969.
- Allen, P.J., Polizzi, G., Krakow, K., Fish, D.R., Lemieux, L., 1998. Identification of EEG events in the MR scanner: the problem of pulse artifact and a method for its subtraction. *NeuroImage* 8, 229–239.
- Allen, P.J., Josephs, O., Turner, R., 2000. A method for removing imaging artifact from continuous EEG recorded during functional MRI. *NeuroImage* 12, 230–239.
- Amjad, A.M., Halliday, D.M., Rosenberg, J.R., Conway, B.A., 1997. An extended difference of coherence test for comparing and combining several independent coherence estimates: theory and application to the study of motor units and physiological tremor. *J. Neurosci. Methods* 73, 69–79.
- Anghinah, R., Caramelli, P., Takahashi, D.Y., Nitrini, R., Sameshima, K., 2005. EEG alpha band coherence analysis in healthy adults: preliminary results. *Arq. Neuropsiquiatr.* 63, 83–86.

- Arnold, N., Tapio, S., 2001. Estimation of Parameters and Eigenmodes of Multivariate Autoregressive Models. *ACM* 27–57.
- Babiloni, C., Babiloni, F., Carducci, F., Cincotti, F., Vecchio, F., Cola, B., Rossi, S., Miniussi, C., Rossini, P.M., 2004. Functional frontoparietal connectivity during short-term memory as revealed by high-resolution EEG coherence analysis. *Behav. Neurosci.* 118, 687–697.
- Barry, R.J., Clarke, A.R., McCarthy, R., Selikowitz, M., Johnstone, S.J., Rushby, J.A., 2004. Age and gender effects in EEG coherence: I. Developmental trends in normal children. *Clin. Neurophysiol.* 115, 2252–2258.
- Barry, R.J., Clarke, A.R., McCarthy, R., Selikowitz, M., 2005. Adjusting EEG coherence for inter-electrode distance effects: an exploration in normal children. *Int. J. Psychophysiol.* 55, 313–321.
- Barry, R.J., Clarke, A.R., McCarthy, R., Selikowitz, M., 2009. EEG coherence in children with attention-deficit/hyperactivity disorder and comorbid reading disabilities. *Int. J. Psychophysiol.* 71, 205–210.
- Beaumont, J.G., Mayes, A.R., Rugg, M.D., 1978. Asymmetry in EEG alpha coherence and power: effects of task and sex. *Electroencephalogr. Clin. Neurophysiol.* 45, 393–401.
- Berger, H., 1930. Über das Elektroenkephalogramm des Menschen II. *J. Psychol. Neurol.* 40, 160–179.
- Brem, S., Bach, S., Kucian, K., Guttorm, T.K., Martin, E., Lyytinen, H., Brandeis, D., Richardson, U., 2010. Brain sensitivity to print emerges when children learn letter-speech sound correspondences. *Proc. Natl. Acad. Sci. U. S. A.* 107, 7939–7944.
- Butz, M., Timmermann, L., Gross, J., Pollok, B., Dirks, M., Hefter, H., Schnitzler, A., 2006. Oscillatory coupling in writing and writer's cramp. *J. Physiol. Paris* 99, 14–20.
- Chugani, H.T., Phelps, M.E., Mazziotta, J.C., 1987. Positron emission tomography study of human brain functional development. *Ann. Neurol.* 22, 487–497.
- Clarke, A.R., Barry, R.J., Heaven, P.C., McCarthy, R., Selikowitz, M., Byrne, M.K., 2008. EEG coherence in adults with attention-deficit/hyperactivity disorder. *Int. J. Psychophysiol.* 67, 35–40.
- De Munck, J.C., 2002. A linear discretization of the volume conductor boundary integral equation using analytically integrated elements (electrophysiology application). *IEEE Trans. Biomed. Eng.* 39, 986–990.
- Delorme, A., Makeig, S., 2004. EEGLAB: an open source toolbox for analysis of single-trial EEG dynamics including independent component analysis. *J. Neurosci. Methods* 134, 9–21.
- Ding, M., Bressler, S.L., Yang, W., Liang, H., 2000. Short-window spectral analysis of cortical event-related potentials by adaptive multivariate autoregressive modeling: data preprocessing, model validation, and variability assessment. *Biol. Cybern.* 83, 35–45.
- Doppelmayr, M., Klimesch, W., Pachinger, T., Ripper, B., 1998. Individual differences in brain dynamics: important implications for the calculation of event-related band power. *Biol. Cybern.* 79, 49–57.
- Dosenbach, N.U., Nardos, B., Cohen, A.L., Fair, D.A., Power, J.D., Church, J.A., Nelson, S.M., Wig, G.S., Vogel, A.C., Lessov-Schlaggar, C.N., Barnes, K.A., Dubis, J.W., Feczko, E., Coalson, R.S., Pruett Jr., J.R., Barch, D.M., Petersen, S.E., Schlaggar, B.L., 2010a. Prediction of individual brain maturity using fMRI. *Science* 329, 1358–1361.
- Dosenbach, N.U., Nardos, B., Cohen, A.L., Fair, D.A., Power, J.D., Church, J.A., Nelson, S.M., Wig, G.S., Vogel, A.C., Lessov-Schlaggar, C.N., Barnes, K.A., Dubis, J.W., Feczko, E., Coalson, R.S., Pruett Jr., J.R., Barch, D.M., Petersen, S.E., Schlaggar, B.L., 2010b. Prediction of individual brain maturity using fMRI. *Science* 329, 1358–1361.
- Dubovik, S., Pignat, J.M., Ptak, R., Abouafia, T., Allet, L., Gillibert, N., Magnin, C., Albert, F., Momjian-Mayor, I., Nahum, L., Lascano, A.M., Michel, C.M., Schneider, A., Guggisberg, A.G., 2012. The behavioral significance of coherent resting-state oscillations after stroke. *NeuroImage* 61, 249–257.
- Essl, M., Rappelsberger, P., 1998. EEG coherence and reference signals: experimental results and mathematical explanations. *Med. Biol. Eng. Comput.* 36, 399–406.
- Fair, D.A., Dosenbach, N.U., Church, J.A., Cohen, A.L., Brahmbhatt, S., Miezin, F.M., Barch, D.M., Raichle, M.E., Petersen, S.E., Schlaggar, B.L., 2007. Development of distinct control networks through segregation and integration. *Proc. Natl. Acad. Sci. U. S. A.* 104, 13507–13512.
- Fair, D.A., Cohen, A.L., Dosenbach, N.U., Church, J.A., Miezin, F.M., Barch, D.M., Raichle, M.E., Petersen, S.E., Schlaggar, B.L., 2008. The maturing architecture of the brain's default network. *Proc. Natl. Acad. Sci. U. S. A.* 105, 4028–4032.
- Fein, G., Raz, J., Brown, F.F., Merrin, E.L., 1988. Common reference coherence data are confounded by power and phase effects. *Electroencephalogr. Clin. Neurophysiol.* 69, 581–584.
- Feinberg, I., Campbell, I.G., 2010. Sleep EEG changes during adolescence: an index of a fundamental brain reorganization. *Brain Cogn.* 72, 56–65.
- Fuchs, M., Wagner, M., Kastner, J., 2007. Development of volume conductor and source models to localize epileptic foci. *J. Clin. Neurophysiol.* 24, 101–119.
- Gasser, T., Jennen-Steinmetz, C., Verleger, R., 1987. EEG coherence at rest and during a visual task in two groups of children. *Electroencephalogr. Clin. Neurophysiol.* 67, 151–158.
- Gasser, T., Verleger, R., Bacher, P., Sroka, L., 1988. Development of the EEG of school-age children and adolescents. I. Analysis of band power. *Electroencephalogr. Clin. Neurophysiol.* 69, 91–99.
- Gasser, T., Rousson, V., Schreier Gasser, U., 2003. EEG power and coherence in children with educational problems. *J. Clin. Neurophysiol.* 20, 273–282.
- Gogtay, N., Giedd, J.N., Lusk, L., Hayashi, K.M., Greenstein, D., Vaituzis, A.C., Nugent 3rd, T.F., Herman, D.H., Clasen, L.S., Toga, A.W., Rapoport, J.L., Thompson, P.M., 2004. Dynamic mapping of human cortical development during childhood through early adulthood. *Proc. Natl. Acad. Sci. U. S. A.* 101, 8174–8179.
- Goldman, R.I., Stern, J.M., Engel Jr., J., Cohen, M.S., 2002. Simultaneous EEG and fMRI of the alpha rhythm. *Neuroreport* 13, 2487–2492.
- Grasman, R.P., Huizenga, H.M., Waldorp, L.J., Bocker, K.B., Molenaar, P.C., 2004. Frequency domain simultaneous source and source coherence estimation with an application to MEG. *IEEE Trans. Biomed. Eng.* 51, 45–55.
- Groeschel, S., Vollmer, B., King, M.D., Connelly, A., 2010. Developmental changes in cerebral grey and white matter volume from infancy to adulthood. *Int. J. Dev. Neurosci.* 28, 481–489.
- Gross, J., Kujala, J., Hamalainen, M., Timmermann, L., Schnitzler, A., Salmelin, R., 2001. Dynamic imaging of coherent sources: studying neural interactions in the human brain. *Proc. Natl. Acad. Sci. U. S. A.* 98, 694–699.
- Gross, J., Timmermann, L., Kujala, J., Dirks, M., Schnitzler, A., Salmelin, R., Schnitzler, A., 2002. The neural basis of intermittent motor control in humans. *Proc. Natl. Acad. Sci. U. S. A.* 99, 2299–2302.
- Hallez, H., Vanrumste, B., Grech, R., Muscat, J., De Clercq, W., Vergult, A., D'Asseler, Y., Camilleri, K.P., Fabri, S.G., Van Huffel, S., Lemahieu, I., 2007. Review on solving the forward problem in EEG source analysis. *J. Neuroeng. Rehabil.* 4, 46.
- Haufe, S., Nikulin, V.V., Müller, K.R., Nolte, G., 2013. A critical assessment of connectivity measures for EEG data: a simulation study. *NeuroImage* 64, 120–133.
- Hillebrand, A., Singh, K.D., Holliday, I.E., Furlong, P.L., Barnes, G.R., 2005. A new approach to neuroimaging with magnetoencephalography. *Hum. Brain Mapp.* 25, 199–211.
- Hoekema, R., Wieneke, G.H., Leijten, F.S., van Veelen, C.W., van Rijen, P.C., Huiskamp, G.J., Ansems, J., van Huffelen, A.C., 2003. Measurement of the conductivity of skull, temporarily removed during epilepsy surgery. *Brain Topogr.* 16, 29–38.
- Huttenlocher, P.R., 1990. Morphometric study of human cerebral cortex development. *Neuropsychologia* 28, 517–527.
- Jung, T.P., Makeig, S., Westerfield, M., Townsend, J., Courchesne, E., Sejnowski, T.J., 2000. Removal of eye activity artifacts from visual event-related potentials in normal and clinical subjects. *Clin. Neurophysiol.* 111, 1745–1758.
- Kaminski, M., Ding, M., Truccolo, W.A., Bressler, S.L., 2001. Evaluating causal relations in neural systems: granger causality, directed transfer function and statistical assessment of significance. *Biol. Cybern.* 85, 145–157.
- Knyazeva, M.G., Kurganskaya, M.E., Kurgansky, A.V., Njokiktjen, C.J., Vildavsky, V.J., 1994. Interhemispheric interaction in children of 7–8: analysis of EEG coherence and finger tapping parameters. *Behav. Brain Res.* 61, 47–58.
- Krause, V., Schnitzler, A., Pollok, B., 2010. Functional network interactions during sensorimotor synchronization in musicians and non-musicians. *NeuroImage* 52, 245–251.
- Kujala, J., Gross, J., Salmelin, R., 2008. Localization of correlated network activity at the cortical level with MEG. *NeuroImage* 39, 1706–1720.
- Laufs, H., 2008. Endogenous brain oscillations and related networks detected by surface EEG-combined fMRI. *Hum. Brain Mapp.* 29, 762–769.
- Laufs, H., Kleinschmidt, A., Beyerle, A., Eger, E., Salek-Haddadi, A., Preibisch, C., Krakow, K., 2003. EEG-correlated fMRI of human alpha activity. *NeuroImage* 19, 1463–1476.
- Laufs, H., Holt, J.L., Elfont, R., Krams, M., Paul, J.S., Krakow, K., Kleinschmidt, A., 2006. Where the BOLD signal goes when alpha EEG leaves. *NeuroImage* 31, 1408–1418.
- Lehmann, D., Skrandies, W., 1980. Reference-free identification of components of checkerboard-evoked multichannel potential fields. *Electroencephalogr. Clin. Neurophysiol.* 48, 609–621.
- Liljestrom, M., Kujala, J., Jensen, O., Salmelin, R., 2005. Neuromagnetic localization of rhythmic activity in the human brain: a comparison of three methods. *NeuroImage* 25, 734–745.
- Littow, H., Elseoud, A.A., Haapea, M., Isohanni, M., Moilanen, I., Mankinen, K., Nikkinen, J., Rahko, J., Rantala, H., Remes, J., Starck, T., Tervonen, O., Veijola, J., Beckmann, C., Kiviniemi, V.J., 2010. Age-related differences in functional nodes of the brain cortex – a high model order group ICA study. *Front. Syst. Neurosci.* 4.
- Liu, Z., Fukunaga, M., de Zwart, J.A., Duyn, J.H., 2010. Large-scale spontaneous fluctuations and correlations in brain electrical activity observed with magnetoencephalography. *NeuroImage* 51, 102–111.
- Lopes da Silva, F.H., Hoeks, A., Smits, H., Zetterberg, L.H., 1974. Model of brain rhythmic activity. The alpha-rhythm of the thalamus. *Kybernetik* 15, 27–37.
- Lüchinger, R., Michels, L., Martin, E., Brandeis, D., 2011. EEG-BOLD correlations during (post-)adolescent brain maturation. *NeuroImage* 56 (3), 1493–1505.
- Lüchinger, R., Michels, L., Martin, E., Brandeis, D., 2012. Brain state regulation during normal development: intrinsic activity fluctuations in simultaneous EEG-fMRI. *NeuroImage* 60, 1426–1439.
- Mantini, D., Perrucci, M.G., Del Gratta, C., Romani, G.L., Corbetta, M., 2007. Electrophysiological signatures of resting state networks in the human brain. *Proc. Natl. Acad. Sci. U. S. A.* 104, 13170–13175.
- Marosi, E., Harmony, T., Sanchez, L., Becker, J., Bernal, J., Reyes, A., Diaz de Leon, A.E., Rodriguez, M., Fernandez, T., 1992. Maturation of the coherence of EEG activity in normal and learning-disabled children. *Electroencephalogr. Clin. Neurophysiol.* 83, 350–357.
- McLaughlin, N.C., Paul, R.H., Grieve, S.M., Williams, L.M., Laidlaw, D., DiCarlo, M., Clark, C.R., Whelihan, W., Cohen, R.A., Whitford, T.J., Gordon, E., 2007. Diffusion tensor imaging of the corpus callosum: a cross-sectional study across the lifespan. *Int. J. Dev. Neurosci.* 25, 215–221.
- Michels, L., Lüchinger, R., Koenig, T., Martin, E., Brandeis, D., 2012. Developmental changes of BOLD signal correlations with global human EEG power and synchronization during working memory. *PLoS One* 7.
- Mills, K.L., Bathula, D., Dias, T.G., Iyer, S.P., Fenesy, M.C., Musser, E.D., Stevens, C.A., Thurlow, B.L., Carpenter, S.D., Nagel, B.J., Nigg, J.T., Fair, D.A., 2012. Altered cortico-striatal-thalamic connectivity in relation to spatial working memory capacity in children with ADHD. *Front Psychiatry* 3 (2). <http://dx.doi.org/10.3389/fpsy.2012.00002> (Electronic publication ahead of print, 2012 Jan 25).
- Mizuhara, H., Wang, L.Q., Kobayashi, K., Yamaguchi, Y., 2005. Long-range EEG phase synchronization during an arithmetic task indexes a coherent cortical network simultaneously measured by fMRI. *NeuroImage* 27, 553–563.
- Moeller, F., Muthuraman, M., Stephani, U., Deuschl, G., Raethjen, J., Siniatchkin, M., 2012. Dynamic imaging of coherent sources in absences and generalized photoparoxysmal responses – a comparison with EEG-fMRI studies. *Hum. Brain Mapp.*

- Moosmann, M., Ritter, P., Krastel, I., Brink, A., Thees, S., Blankenburg, F., Taskin, B., Obrig, H., Villringer, A., 2003. Correlates of alpha rhythm in functional magnetic resonance imaging and near infrared spectroscopy. *NeuroImage* 20, 145–158.
- Muller, V., Gruber, W., Klimesch, W., Lindenberger, U., 2009. Lifespan differences in cortical dynamics of auditory perception. *Dev. Sci.* 12, 839–853.
- Muthuraman, M., Raethjen, J., Hellriegel, H., Deuschl, G., Heute, U., 2008. Imaging coherent sources of tremor related EEG activity in patients with Parkinson's disease. *Conf. Proc. IEEE Eng. Med. Biol. Soc.* 2008, 4716–4719.
- Muthuraman, M., Heute, U., Deuschl, G., Raethjen, J., 2010. The central oscillatory network of essential tremor. *Conf. Proc. IEEE Eng. Med. Biol. Soc.* 1, 154–157.
- Muthuraman, M., Heute, U., Arning, K., Anwar, A.R., Elble, R., Deuschl, G., Raethjen, J., 2012a. Oscillating central motor networks in pathological tremors and voluntary movements. What makes the difference? *NeuroImage* 60, 1331–1339.
- Muthuraman, M., Tamas, G., Hellriegel, H., Deuschl, G., Raethjen, J., 2012b. Source analysis of beta-synchronisation and cortico-muscular coherence after movement termination based on high resolution electroencephalography. *PLoS One* 7, e33928.
- Nolte, G., Bai, O., Wheaton, L., Mari, Z., Vorbach, S., Hallett, M., 2004. Identifying true brain interaction from EEG data using the imaginary part of coherency. *Clin. Neurophysiol.* 115, 2292–2307.
- Oostenveld, R., Fries, P., Maris, E., Schoffelen, J.M., 2011. FieldTrip: open source software for advanced analysis of MEG, EEG, and invasive electrophysiological data. *J. Intell. Neurosci.* 2011, 1–9.
- Pascual-Marqui, R.D., Sekihara, K., Brandeis, D., Michel, C.M., 2009. Imaging the electric neuronal generators of EEG/MEG. In: Michel, C.M., Brandeis, T.K.D., Gianotti, L.R.R., Wackermann, J. (Eds.), *Electrical Neuroimaging*. Cambridge University Press, Cambridge.
- Pollok, B., Krause, V., Butz, M., Schnitzler, A., 2009. Modality specific functional interaction in sensorimotor synchronization. *Hum. Brain Mapp.* 30, 1783–1790.
- Rosenberg, J.R., Amjad, A.M., Breeze, P., Brillinger, D.R., Halliday, D.M., 1989. The Fourier approach to the identification of functional coupling between neuronal spike trains. *Prog. Biophys. Mol. Biol.* 53, 1–31.
- Sameshima, K., Baccala, L.A., 1999. Using partial directed coherence to describe neuronal ensemble interactions. *J. Neurosci. Methods* 94, 93–103.
- Sauseng, P., Klimesch, W., Schabus, M., Doppelmayr, M., 2005. Fronto-parietal EEG coherence in theta and upper alpha reflect central executive functions of working memory. *Int. J. Psychophysiol.* 57, 97–103.
- Schack, B., Grieszbach, G., Nowak, H., Krause, W., 1999. The sensitivity of instantaneous coherence for considering elementary comparison processing. Part II: similarities and differences between EEG and MEG coherences. *Int. J. Psychophysiol.* 31, 241–259.
- Scheeringa, R., Bastiaansen, M.C., Petersson, K.M., Oostenveld, R., Norris, D.G., Hagoort, P., 2008. Frontal theta EEG activity correlates negatively with the default mode network in resting state. *Int. J. Psychophysiol.* 67, 242–251.
- Schellberg, D., Besthorn, C., Klos, T., Gasser, T., 1990. EEG power and coherence while male adults watch emotional video films. *Int. J. Psychophysiol.* 9, 279–291.
- Schelter, B., Timmer, J., Eichler, M., 2009. Assessing the strength of directed influences among neural signals using renormalized partial directed coherence. *J. Neurosci. Methods* 179, 121–130.
- Schoffelen, J.M., Oostenveld, R., Fries, P., 2008. Imaging the human motor system's beta-band synchronization during isometric contraction. *NeuroImage* 41, 437–447.
- Segalowitz, S.J., Santesso, D.L., Jetha, M.K., 2010. Electrophysiological changes during adolescence: a review. *Brain Cogn.* 72, 86–100.
- Sekihara, K., Scholz, B., 1996. Generalized Wiener estimation of three-dimensional current distribution from biomagnetic measurements. *IEEE Trans. Biomed. Eng.* 43, 281–291.
- Sekihara, K., Owen, J.P., Trisno, S., Nagarajan, S.S., 2011. Removal of spurious coherence in MEG source-space coherence analysis. *IEEE Trans. Biomed. Eng.* 58, 3121–3129.
- Singer, W., 2009. Distributed processing and temporal codes in neuronal networks. *Cogn. Neurodyn.* 3, 189–196.
- Srinivasan, R., Nunez, P.L., Silberstein, R.B., 1998. Spatial filtering and neocortical dynamics: estimates of EEG coherence. *IEEE Trans. Biomed. Eng.* 45, 814–826.
- Srinivasan, R., Winter, W.R., Ding, J., Nunez, P.L., 2007. EEG and MEG coherence: measures of functional connectivity at distinct spatial scales of neocortical dynamics. *J. Neurosci. Methods* 166, 41–52.
- Steriade, M., Deschenes, M., 1984. The thalamus as a neuronal oscillator. *Brain Res.* 320, 1–63.
- Steriade, M., Llinas, R.R., 1988. The functional states of the thalamus and the associated neuronal interplay. *Physiol. Rev.* 68, 649–742.
- Stevens, M.C., 2009. The developmental cognitive neuroscience of functional connectivity. *Brain Cogn.* 70, 1–12.
- Sudmeyer, M., Pollok, B., Hefter, H., Gross, J., Butz, M., Wojtecki, L., Timmermann, L., Schnitzler, A., 2006. Synchronized brain network underlying postural tremor in Wilson's disease. *Mov. Disord.* 21, 1935–1940.
- Supekar, K., Uddin, L.Q., Prater, K., Amin, H., Greicius, M.D., Menon, V., 2010. Development of functional and structural connectivity within the default mode network in young children. *NeuroImage* 52, 290–301.
- Takigawa, M., Wang, G., Kawasaki, H., Fukuzako, H., 1996. EEG analysis of epilepsy by directed coherence method. A data processing approach. *Int. J. Psychophysiol.* 21, 65–73.
- Tapio, S., Arnold, N., 2001. Algorithm 808: Arfit—A Matlab Package for the Estimation of Parameters and Eigenmodes of Multivariate Autoregressive Models. *ACM* 58–65.
- Tarokh, L., Carskadon, M.A., Achermann, P., 2010. Developmental changes in brain connectivity assessed using the sleep EEG. *Neuroscience* 171, 622–634.
- Thatcher, R.W., Krause, P.J., Hrybyk, M., 1986. Cortico-cortical associations and EEG coherence: a two-compartmental model. *Electroencephalogr. Clin. Neurophysiol.* 64, 123–143.
- Thatcher, R.W., Walker, R.A., Giudice, S., 1987. Human cerebral hemispheres develop at different rates and ages. *Science* 236, 1110–1113.
- Timmermann, L., Gross, J., Dirks, M., Volkmann, J., Freund, H.J., Schnitzler, A., 2003. The cerebral oscillatory network of Parkinsonian resting tremor. *Brain* 126, 199–212.
- Tucker, D.M., Roth, D.L., Bair, T.B., 1986. Functional connections among cortical regions: topography of EEG coherence. *Electroencephalogr. Clin. Neurophysiol.* 63, 242–250.
- van Albada, S.J., Kerr, C.C., Chiang, A.K., Rennie, C.J., Robinson, P.A., 2010. Neurophysiological changes with age probed by inverse modeling of EEG spectra. *Clin. Neurophysiol.* 121, 21–38.
- Van der Werf, Y.D., Scheltens, P., Lindeboom, J., Witter, M.P., Uylings, H.B., Jolles, J., 2003. Deficits of memory, executive functioning and attention following infarction in the thalamus; a study of 22 cases with localised lesions. *Neuropsychologia* 41, 1330–1344.
- van Uiter, R., Johnson, C., 2000. Can a spherical model substitute for a realistic model in forward and inverse MEG simulations. *Biomagnetism J.* 1, 1–3.
- Van Veen, B.D., Van Drongelen, W., Yuchtman, M., Suzuki, A., 2002. Localization of brain electrical activity via linearly constrained minimum variance spatial filtering. *IEEE Trans. Biomed. Eng.* 44, 867–880.
- Varotto, G., Franceschetti, S., Spreafico, R., Tassi, L., Panzica, F., 2010. Partial directed coherence estimated on stereo-EEG signals in patients with Taylor's type focal cortical dysplasia. *Conf. Proc. IEEE Eng. Med. Biol. Soc.* 2010, 4646–4649.
- Wang, G., Takigawa, M., 1992. Directed coherence as a measure of interhemispheric correlation of EEG. *Int. J. Psychophysiol.* 13, 119–128.
- Whitford, T.J., Rennie, C.J., Grieve, S.M., Clark, C.R., Gordon, E., Williams, L.M., 2007. Brain maturation in adolescence: concurrent changes in neuroanatomy and neurophysiology. *Hum. Brain Mapp.* 28, 228–237.
- Yakovlev, P.I., Lecours, A.R., 1967. *The Myelogenetic Cycles of Regional Maturation of the Brain*. Blackwell Scientific, Oxford.